ARTICLE

OBC
www.rsc.org/obc

Do the interstellar molecules CCCO and CCCS rearrange when energised?

Khoa Minh Tran, Andrew M. McAnoy and John H. Bowie
Department of Chemistry, The University of Adelaide, South Australia, 5005

Received 23rd December 2003, Accepted 6th February 2004
First published as an Advance Article on the web 27th February 2004

Neutrals CCCO, $CC^{13}CO$, CCCS and $CC^{13}CS$ have been prepared by one-electron vertical (Franck–Condon) oxidation of the precursor anion radicals $(CCCO)^{-\bullet}$, $(CC^{13}CO)^{-\bullet}$, $(CCCS)^{-\bullet}$ and $(CC^{13}CS)^{-\bullet}$ respectively in collision cells of a reverse sector mass spectrometer. Ionisation of the neutrals to decomposing cations shows the neutrals to be stable for the microsecond duration of the neutralisation–ionisation ($^{-}NR^{+}$) experiment. No rearrangement of the label in energised $CC^{13}CO$ or $CC^{13}CS$ occurs during these experiments. In contrast, minor rearrangement of $(CC^{13}CO)^{+\bullet}$ is observed [$(CC^{13}CO)^{+\bullet} \longrightarrow (OCC^{13}C)^{+\bullet}$], while significant rearrangement occurs for $(CC^{13}CS)^{+\bullet}$ [$(CC^{13}CS)^{+\bullet} \longrightarrow (SCC^{13}C)^{+\bullet}$]. Theoretical calculations at the CCSD(T)/aug-cc-pVDZ//B3LYP/6-31G(d) level of theory show that the cationic rearrangements occur by stepwise processes *via* key rhombic structures. Overall, the degenerate processes result in O and S migration from C-3 to C-1. The cations $(CCCO)^{+\bullet}$ and $(CCCS)^{+\bullet}$ require excess energies of ≥ 516 and ≥ 226 kJ mol^{-1} respectively to effect rearrangement.

Introduction

Small cumulenes and heterocumulenes may be formed by neutralisation–ionisation processes ($^{-}NR^{+}$) from anions in a reverse sector mass spectrometer equipped with a dual collision cell assembly.[1] One of the interesting features of these experiments is when these neutrals are energised, some may undergo rearrangement of the carbon skeleton. Particular examples of this behaviour are (i) CCCC[2] and CCCCC,[3] both of which undergo randomisation of the carbon atoms *via* rhombic intermediates, and (ii) NCCCN, which scrambles both N and C.[4]

Many cumulenes and heterocumulenes have been detected in interstellar dust clouds, and in circumstellar envelopes of carbon-rich suns.[5–9] Two of the most abundant heterocumulenes to be reported are CCCO and CCCS. Sulfur compounds are particularly interesting since they are often more abundant than their oxygen analogues, even though the cosmic abundance of sulfur is less than that of oxygen.[10–12]

The aim of this study is to make $CC^{13}CO$ and $CC^{13}CS$, and, using the neutralisation–reionisation ($^{-}NR^{+}$) technique as a probe, to determine whether any rearrangement occurs for energised neutrals. We are interested in comparing these two systems for two reasons: (i) because of the cumulene rearrangements described above, and (ii) because rearrangements occur for the related systems CCCHO and CCCHS. In the former case, CCCHO rearranges to HCCCO by H rearrangement,[13] whereas CCCHS rearranges to HCCCS by competitive H and S rearrangement.[14] Perhaps CCCS may undergo S rearrangement, but CCCO will be stable?

Neutral CCCO has been detected [together with the related propynal (HC≡C–CHO), from which CCCO may be formed] in the dark molecular cloud TMC-1.[15] It has been made by a number of methods,[16–19] including neutralisation of $[CCCO]^{+\bullet}$[17] and $[CCCO]^{-\bullet}$.[19] A number of theoretical studies have been devoted to cumulene oxides (including CCCO),[20–25] and their rotational spectra have been measured.[26,27] There are two stable forms of CCCO: the $^{1}\Sigma$ singlet ground state is linear,[27] while the $^{3}A'$ triplet state is bent and 271 kJ less stable than the ground state singlet (at the RCCSD(T)/aug-cc-pVDZ//B3LYP/6-31+G* level of theory).[19]

Sulfur carbon clusters occur in both dark clouds and circumstellar envelopes.[28–30] Neutral CCCS has been detected in the circumstellar envelope of the star IRC+10216[31,32] and has been synthesised in the laboratory.[32,33] A number of theoretical studies on CCCS have been reported,[28,29,32,34] and it has been proposed that CCCS may be formed from the interstellar radical CCCH, as shown in eqn. (1).[34]

$$CCCH^{\bullet} + S \longrightarrow CCCS + H^{\bullet} \qquad (1)$$

Results and discussion

Syntheses of the anion precursors

The most important part of this project involves the synthesis of the precursor neutrals which will be used to make $(CCCO)^{-\bullet}$, $(CCCS)^{-\bullet}$ and their labelled analogues $(CC^{13}CO)^{-\bullet}$ and $(CC^{13}CS)^{-\bullet}$. In our previous synthesis of $(CCCO)^{-\bullet}$, we used TMSC≡C–CO–Et as the precursor neutral. This is not suitable for the preparation of ^{13}C labelled precursors, so we undertook the synthetic procedures shown in Scheme 1.

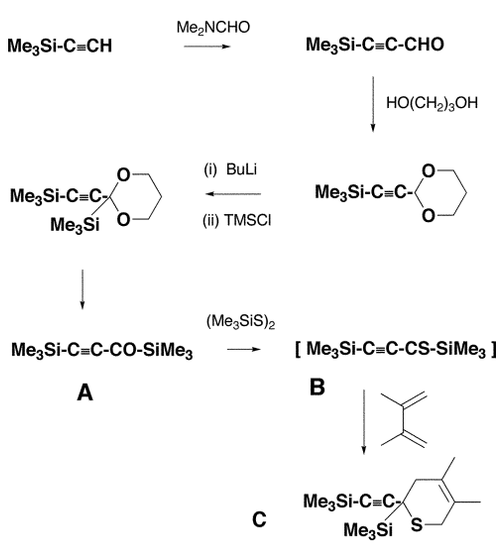

Scheme 1

The syntheses commence with the TMS derivative of acetylene, which is allowed to react with dimethylformamide to yield the aldehyde. The aldehyde is converted to the acetal which on base treatment allows the addition of the second TMS group. Hydrolysis of the acetal furnishes the bis TMS ketone **A**, which

DOI: 10.1039/b316867k

is the precursor of $(CCCO)^{-\bullet}$. The ketone **A** can be converted into the thioketone **B** by reaction with bis TMS disulfide. However the thioketone **B** is unstable, and is trapped *in situ* to form the Diels–Alder adduct **C**. This species is used (as shown below) to produce $(CCCS)^{-\bullet}$. The same sequence was used for the formation of the two ^{13}C labelled precursor molecules. The label is introduced in the first step of the synthesis, *i.e.* by the reaction between TMS acetylene and $Me_2N^{13}CHO$.

Syntheses and stabilities of $(CCCO)^{-\bullet}$ and $(CCCS)^{-\bullet}$ and their labelled analogues

These species are formed from **A** and **C** as shown in Scheme 2. In essence, for eqn. (2), F^- ions, formed from SF_6 on electron capture, effect two $S_N2(Si)$ reactions to produce the required $(CCCO)^{-\bullet}$. This procedure is an adaptation (using $SF_6{}^2$) of a method first reported by Squires[35] for systems containing two TMS groups. Equation (2) shows only reactants and products: the actual sequence of the double de-silylation process is not known.[35] The process forming $(CCCS)^{-\bullet}$ [eqn. (3)] is similar except that a retro Diels–Alder process accompanies the desilylation steps. The sequence of the steps in the formation of $(CCCS)^{-\bullet}$ is not known.

$$Me_3Si\text{-}C{\equiv}C\text{-}CO\text{-}SiMe_3 + 2SF_6 \xrightarrow{e} (CCCO)^{-\bullet} + 2Me_3SiF + 2SF_4 \quad (2)$$

A

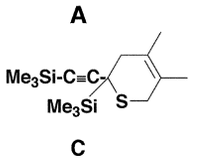

$$+ 2SF_6 \xrightarrow{e} (CCCS)^{-\bullet} + 2Me_3SiF + 2SF_4 + CH_2{=}C(Me)\text{-}C(Me){=}CH_2 \quad (3)$$

C

Scheme 2

Before attempting the one-electron oxidations of $(CCCO)^{-\bullet}$ and $(CCCS)^{-\bullet}$ to the neutrals, it is necessary to be certain that the anions do not rearrange prior to or during the oxidation process. The collision induced mass spectra (MS/MS) of $(CCCO)^{-\bullet}$ and $(CCCS)^{-\bullet}$ show these radical anions to be very stable. The only fragment peaks in the spectra are of very small abundance. They correspond to loss of CO [from $(CCCO)^{-\bullet}$] and the formation of $(CS)^{-\bullet}$ [from $(CCCS)^{-\bullet}$]. The two labelled anions fragment specifically as shown in eqns. (4) and (5). Thus there is no rearrangement of either system when collisionally activated.

$$(CC^{13}CO)^{-\bullet} \longrightarrow (CC)^{-\bullet} + {}^{13}CO \quad (4)$$

$$(CC^{13}CS)^{-\bullet} \longrightarrow ({}^{13}CS)^{-\bullet} + CC \quad (5)$$

Although the above experimental results show that there is no rearrangement of either $(CCCO)^{-\bullet}$ or $(CCCS)^{-\bullet}$ during conditions equivalent to those used for the vertical one-electron oxidations of the anions to the neutrals, it is still of interest to examine theoretically how much excess energy is required to effect oxygen and sulfur rearrangement. These reactions have been studied at the CCSD(T)/aug-cc-pVDZ//B3LYP/6-31G(d) level of theory using Gaussian 98. The results are summarised in Figs. 1 and 2, with full details given in Tables 1 and 2. The lowest energy pathway for degenerate oxygen rearrangement is concerted with a barrier to the transition state of 356 kJ mol^{-1}. This is far too high to allow rearrangement of $(CCCO)^{-\bullet}$ in the first collision cell of the mass spectrometer. The S system is the more complex of the two (see Fig. 2). In this case there is no low-energy concerted reaction. The rearrangement process is a stepwise sequence proceeding through a "rhombic" transition state 219 kJ mol^{-1} above $(CCCS)^{-\bullet}$. This is more energetically favourable than the oxygen rearrangement shown in Fig. 1. Even so, the process is not observed experimentally under conditions of collisional activation.

Table 1 Calculated properties of $CCCO^{-\bullet}$ species shown in Fig. 1

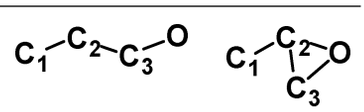

State	$^2A'$	$^2A''$
Relative energy (kJ mol^{-1})[a]	0.0	356.1
Dipole moment (Debye)[b]	3.45	2.96
C_1C_2 (Å)	1.275	1.288
C_2C_3	1.363	1.673
C_1C_3		1.928
C_3O	1.223	1.524
$C_1C_2C_3$ (°)	167.3	80.6
C_2C_3O	142.8	49.3
$C_1C_2C_3O$	180.0	180.0

[a] Energies are calculated at the CCSD(T)/aug-cc-pVDZ//B3LYP/6-31G(d) level of theory and are relative to $CCCO^{-\bullet}$ (−188.9643951 Hartrees). [b] B3LYP/6-31G(d) geometries.

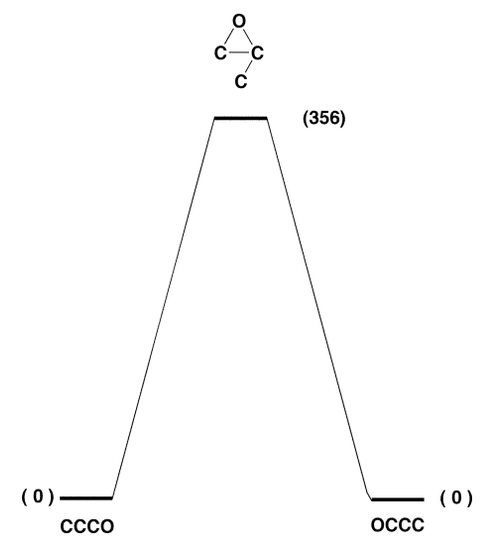

Fig. 1 Degenerate rearrangement of $(CCCO)^{-\bullet}$. Energies [kJ mol^{-1}, relative to $(CCCO)^{-\bullet}$, 0 kJ mol^{-1}] at the CCSD(T)/aug-cc-pVDZ//B3LYP/6-31G(d) level of theory. For details of geometries and energies of minima and transition states see Table 1.

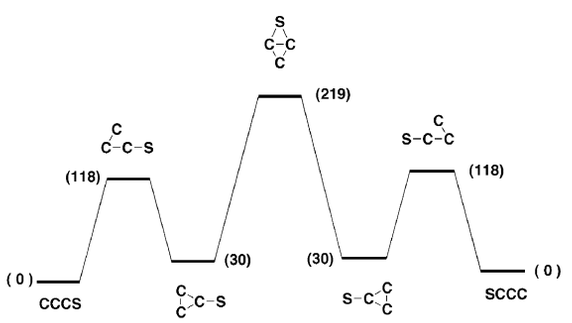

Fig. 2 Degenerate rearrangement of $(CCCS)^{-\bullet}$. Energies [kJ mol^{-1}, relative to $(CCCS)^{-\bullet}$, 0 kJ mol^{-1}] at the CCSD(T)/aug-cc-pVDZ//B3LYP/6-31G(d) level of theory. For details of geometries and energies of minima and transition states see Table 2.

We conclude that the precursor radical anions $(CCCO)^{-\bullet}$ and $(CCCS)^{-\bullet}$ are suitable precursors to effect one-electron oxidation to CCCO and CCCS.

Neutral CCCO and the radical cation $(CCCO)^{+\bullet}$

There are two stable forms of CCCO, the $^1\Sigma$ linear ground state and the $^3A'$ bent triplet state. The difference in energy between the two states has been calculated to be 271 kJ mol^{-1},[19] thus we have not considered the triplet state further. The charge reversal ($^-CR^+$) and neutralisation–reionisation ($^-NR^+$) spectra of

Table 2 Calculated properties of $CCCS^{-\bullet}$ species shown in Fig. 2

	C_1–C_2–C_3–S	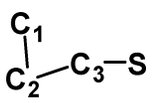	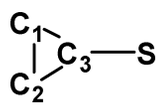	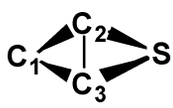
State	$^2\Pi$	—	$^2B_2$	$^2A''$
Relative energy (kJ mol^{-1})[a]	0.0	118.3	30.3	218.7
Dipole moment (Debye)[b]	4.17	2.36	1.59	2.74
C_1C_2 (Å)	1.302	1.334	1.366	1.411
C_2C_3	1.296	1.363	1.427	1.642
C_1C_3		1.935	1.366	1.411
C_3S	1.622	1.631	1.660	1.885
$C_1C_2C_3$ (°)	180.0	91.7	61.4	54.4
C_2C_3S	180.0	167.0	151.4	64.2
$C_1C_2C_3S$	180.0	−67.0	180.0	157.2

[a] Energies are calculated at the CCSD(T)/aug-cc-pVDZ//B3LYP/6-31G(d) level of theory and are relative to $CCCS^{-\bullet}$ (−511.5816670 Hartrees). [b] B3LYP/6-31G(d) geometries.

Table 3 $^-CR^+$ and $^-NR^+$ data for $(CCCO)^{-\bullet}$ and $(CCCS)^{-\bullet}$ [*m/z* (loss) abundance in %]

	$(CCCO)^{-\bullet}$	
	$^-CR^+$	52(parent)100; 40(C)2.3; 36(O)2.9; 28(C_2)1.2; 24(CO)2.0; 12(C_2O)0.2
	$^-NR^+$	52(parent)100; 40(C)2.5; 36(O)2.9; 28(C_2)2.4; 24(CO)2.2; 12(C_2O)0.2
	$(CCCS)^{-\bullet}$	
	$^-CR^+$	68(parent)100; 56(C)10; 44(C_2)3.6; 36(S)0.6; 32(C_3)1.6; 24(CS)0.2
	$^-NR^+$	68(parent)100; 56(C)5.5; 44(C_2)2.5; 36(S)1.5; 32(C_3)1.7; 24(CS)0.2

$(CC^{13}CO)^{-\bullet}$ are shown in Fig. 3: similar data for $(CCCO)^{-\bullet}$ are listed in Table 3. The cation in the CR spectrum is produced by synchronous two-electron oxidation of the anion radical. This spectrum shows exclusive loss of ^{12}C, together with major losses of ^{13}CO and $^{12}C^{12}C$. This indicates that the majority of the decomposing cation radicals have retained the connectivity $(CC^{13}CO)^{+\bullet}$. However, there are minor peaks corresponding to the losses of ^{12}CO and $^{12}C^{13}C$ that are diagnostic to some rearrangement of the cation to $(OCC^{13}C)^{-\bullet}$. The peak areas of these minor peaks (*m/z* 25 and 28) are about 10% of the major peaks (*m/z* 24 and 29). The mechanism of the cation rearrangement will be considered later.

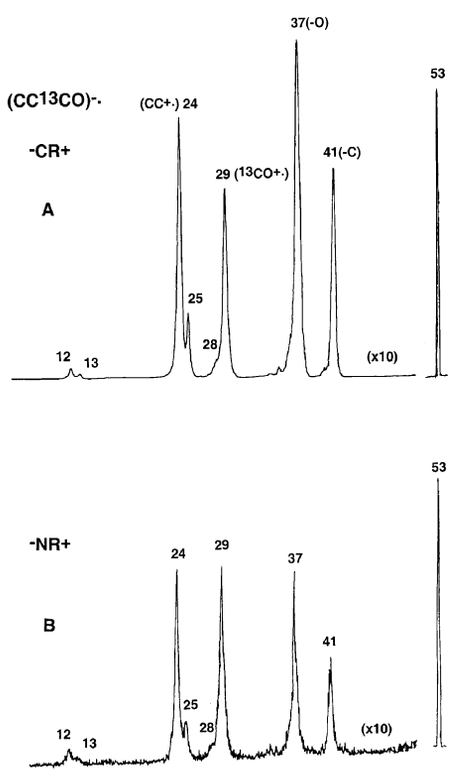

Fig. 3 Spectra of $(CC^{13}CO)^{-\bullet}$: A) $^-CR^+$, B) $^-NR^+$. VG ZAB 2HF mass spectrometer. For experimental conditions see Experimental section.

The $^-NR^+$ spectrum (Fig. 3B) shows a pronounced parent peak (*m/z* 53) which indicates that a portion of the neutrals formed by one-electron oxidation are stable for the period of the NR experiment, *i.e.* ≥ 1 microsecond. The peak ratios of *m/z* 25 to 24 and *m/z* 28 to 29 are slightly less in the $^-NR^+$ spectrum (in comparison to those observed in the $^-CR^+$ spectrum). In addition, *m/z* 29 and 24 are of larger abundance in the $^-NR^+$ spectrum (than the corresponding peaks in the $^-CR^+$ spectrum). If neutral rearrangements occur, *m/z* 25 and 28 would be of greater abundance in the $^-NR^+$ than the $^-CR^+$ spectrum. Since this is not so, the rearrangement peaks observed in the $^-NR^+$ spectrum must originate from the cation, not from neutral $CC^{13}CO$.

The above data show that $CC^{13}CO$ [formed by neutralisation of $(CC^{13}CO)^{-\bullet}$] is a stable species which does not undergo rearrangement during the microsecond duration of the NR experiment. Rearrangement of singlet CCCO has also been studied theoretically at the CCSD(T)/aug-cc-pVDZ//B3LYP/6-31G(d) level of theory. The reaction coordinate is shown in Fig. 4 with full details of all minima and transition states listed in Table 4. There is no low energy concerted process (*cf.* Fig. 1), instead, a high energy stepwise process proceeds through a symmetrical rhombic transition state, which lies 479 kJ mol^{-1} above singlet CCCO. Experiment and theory agree; there is no facile degenerate rearrangement of singlet CCCO.

Why is *m/z* 29 more abundant in the $^-NR^+$ spectrum of $(CC^{13}CO)^{-\bullet}$ (see Figs. 3A and 3B)? The reason for this is apparent when the thermochemistries of the decompositions of CCCO and $(CCCO)^{+\bullet}$ are considered. These are compared in Table 5. The losses of C and O noted in Fig. 3B are high energy decompositions of the cation. The only possible neutral decomposition is loss of CO from CCCO (+334 kJ mol^{-1}). If some of the neutrals have energies ≥ 334 kJ mol^{-1} they may decompose to CC and CO. Thus the enhanced abundance of *m/z* 29 in the $^-NR^+$ spectrum of $(CC^{13}CO)^{-\bullet}$ is due to dissoci-

Table 4 Calculated properties of CCCO neutral species shown in Fig. 4

	C_1–C_2–C_3–O	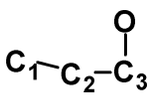	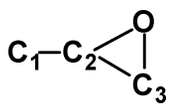	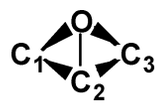
State	$^1\Sigma$	$^1A'$	$^1A'$	$^1A'$
Relative energy (kJ mol^{-1})[a]	0.0	385.6	376.4	478.6
Dipole moment (Debye)[b]	1.95	2.66	1.88	0.55
C_1C_2 (Å)	1.278	1.282	1.296	1.428
C_2C_3	1.299	1.483	1.478	1.428
C_3O	1.161	1.199	1.279	1.467
C_2O		1.876	1.483	1.731
$C_1C_2C_3$ (°)	180.0	174.3	162.8	91.8
C_2C_3O	180.0	88.1	64.6	73.4
$C_1C_2C_3O$	180.0	0.0	180.0	42.2

[a] Energies are calculated at the CCSD(T)/aug-cc-pVDZ//B3LYP/6-31G(d) level of theory and are relative to CCCO (−188.9262679 Hartrees). [b] B3LYP/6-31G(d) geometries.

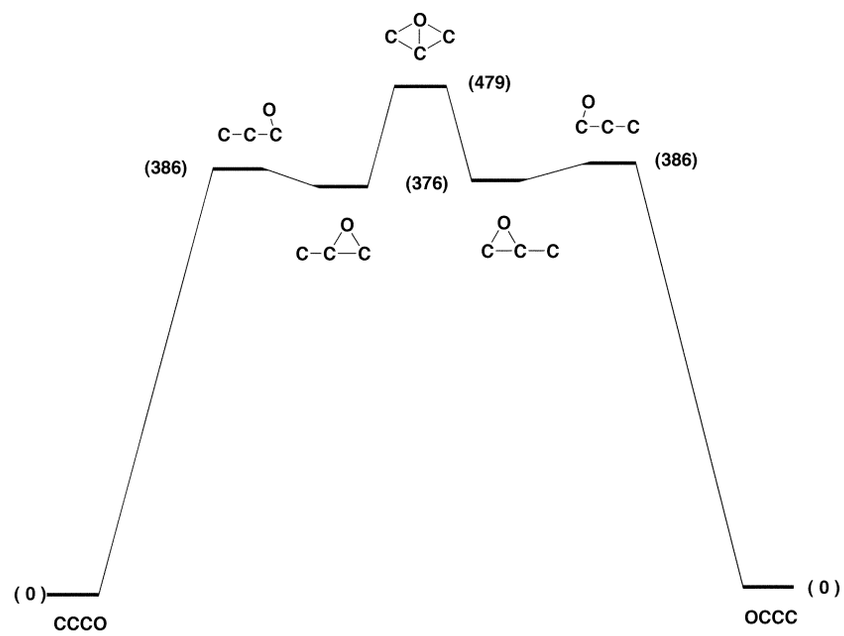

Fig. 4 Degenerate rearrangement of singlet CCCO. Energies [kJ mol^{-1}, relative to CCCO, 0 kJ mol^{-1}] at the CCSD(T)/aug-cc-pVDZ//B3LYP/6-31G(d) level of theory. For details of geometries and energies of minima and transition states see Table 4.

Table 5 Calculated decomposition energies of CCCO neutral and cation[a]

Cation process				Neutral process			
C	+	$CCO^{+\bullet}$	821.7	C	+	CCO	915.2
$C^{+\bullet}$	+	CCO	797.2	CC	+	CO	333.8
$CC^{+\bullet}$	+	CO	465.3	CCC	+	O	887.1
CC	+	$CO^{+\bullet}$	632.1				
$CCC^{+\bullet}$	+	O	996.2				
CCC	+	$O^{+\bullet}$	1264.4				

[a] Calculated at the CCSD(T)/aug-cc-pVDZ//B3LYP/6-31G(d) level of theory.

ation of some neutral $CC^{13}CO$ molecules prior to reionisation. This also explains the smaller abundance of *m*/*z* 28 in the $^-NR^+$ spectrum, since this is only produced following or accompanying rearrangement of the cation.

The $^-CR^+$ and $^-NR^+$ spectra of $(CC^{13}CO)^{-\bullet}$ show that the doublet cation radical $(CC^{13}CO)^{+\bullet}$ does undergo some rearrangement to $(OCC^{13}C)^{+\bullet}$. However this rearrangement is minor, and clearly unfavourable. The cation rearrangement has been investigated theoretically. The process is summarised in Fig. 5 with full details listed in Table 6. The cation rearrangement is quite similar to that already described for the neutral. Energetically, it is less favourable than the neutral rearrangement, requiring a minimum of 516 kJ mol^{-1} to effect the rearrangement. Thus it is not surprising that the cation rearrangement is only a minor process. The cations that rearrange are likely to obtain this excess energy (≥ 516 kJ mol^{-1}) by keV collisions of parent cations occurring subsequent to the Franck–Condon vertical oxidation process.

Neutral CCCS and the radical cation $(CCCS)^{+\bullet}$

The $^-CR^+$ and $^-NR^+$ spectra of $(CC^{13}CS)^{-\bullet}$ are shown in Fig. 6: similar data for $(CCCS)^{-\bullet}$ are recorded in Table 3. The $^-NR^+$ spectrum shows a pronounced peak at *m*/*z* 69, indicating that some of the neutrals are stable for at least a microsecond. The $^-NR^+$ and $^-CR^+$ spectra are similar, with the exception that the peak at *m*/*z* 32 ($S^{+\bullet}$) is of higher abundance in the $^-NR^+$ spectrum. The most important features of the two spectra are that the ratios of the peak areas of *m*/*z* 57 : 56 [$(C^{13}CS)^{+\bullet}$ to $(CCS)^{+\bullet}$] and *m*/*z* 44 : 45 [$(^{13}CS)^{+\bullet}$ to $(CS)^{+\bullet}$] are the same in the two spectra. This means that neutral $CC^{13}CS$ does not rearrange during the microsecond duration of the $^-NR^+$ experiment, and that the rearrangement ions observed in the $^-NR^+$ spectrum are formed by rearrangement of $(CC^{13}CS)^{+\bullet}$. The enhanced peak at *m*/*z* 32 in the $^-NR^+$ spectrum is due to some $CC^{13}CS$ neutrals having sufficient excess energy to effect dissociation to $CC^{13}C$ and S [the exothermicities of the two processes CCCS ⟶ CCC + S and $(CCCS)^{+\bullet}$ ⟶ $(CCC)^{+\bullet}$ + S

Table 6 Calculated properties of $CCCO^{+\bullet}$ species shown in Fig. 5

	C_1–C_2–C_3–O	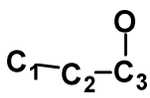	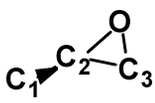	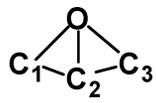
State	$^2\Sigma$	$^2A'$	—	$^2B_2$
Relative energy (kJ mol^{-1})[a]	0.0	431.9	414.9	516.1
Dipole moment (Debye)[b]	2.73	1.38	0.57	2.21
C_1C_2 (Å)	1.221	1.239	1.347	1.389
C_2C_3	1.341	1.500	1.553	1.389
C_3O	1.134	1.217	1.290	1.851
C_2O		1.589	1.383	1.394
$C_1C_2C_3$ (°)	180.0	175.6	151.3	166.8
C_2C_3O	180.0	70.7	57.3	48.4
$C_1C_2C_3O$	180.0	180.0	−139.2	0.0

[a] Energies are calculated at the CCSD(T)/aug-cc-pVDZ//B3LYP/6-31G(d) level of theory and are relative to $CCCO^{+\bullet}$ (−188.5319672 Hartrees). [b] B3LYP/6-31G(d) geometries.

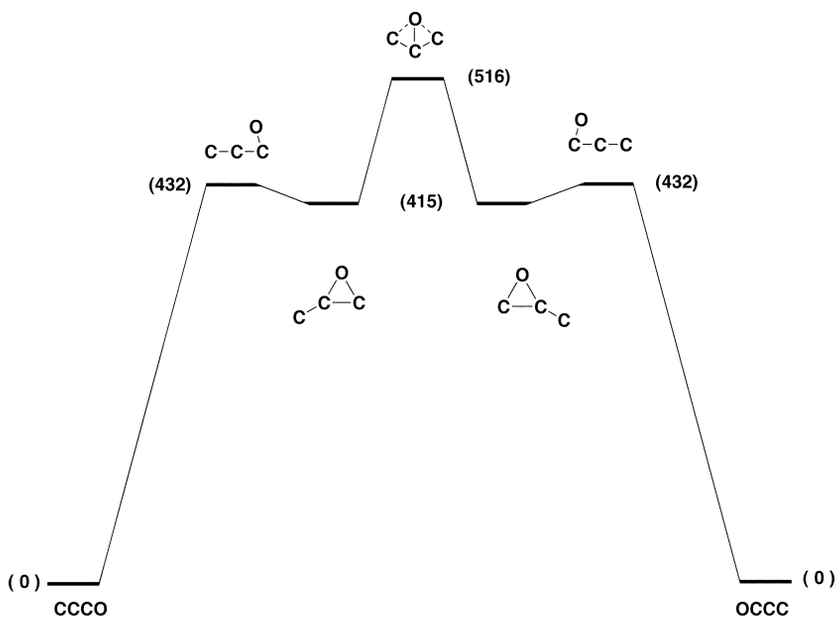

Fig. 5 Degenerate rearrangement of $(CCCO)^{+\bullet}$. Energies [kJ mol^{-1}, relative to $(CCCO)^{+\bullet}$, 0 kJ mol^{-1}] at the CCSD(T)/aug-cc-pVDZ//B3LYP/6-31G(d) level of theory. For details of geometries and energies of minima and transition states see Table 6.

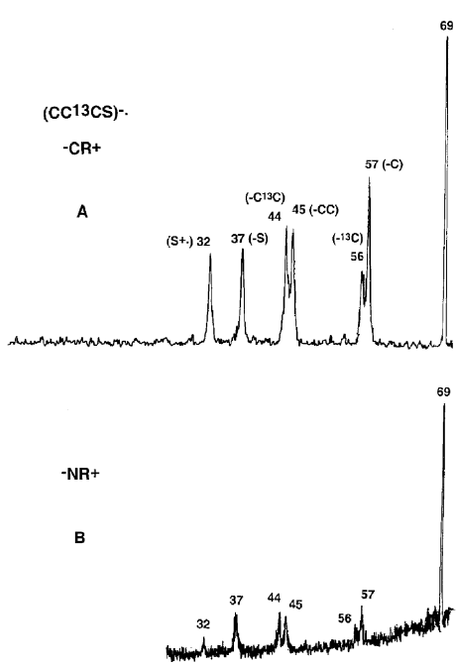

Fig. 6 Spectra of $(CC^{13}CS)^{-\bullet}$: A) $^-CR^+$, B) $^-NR^+$. VG ZAB 2HF mass spectrometer. For experimental conditions see Experimental section.

are +590 and +755 kJ mol^{-1} respectively (at the CCSD(T)/aug-cc-pVDZ//B3LYP/6-31G(d) level of theory)].

The degenerate rearrangements of CCCS and $(CCCS)^{+\bullet}$ have been investigated theoretically. There are two stable forms of CCCS; namely the linear $^1\Sigma$ singlet and the bent triplet. It has been reported[28] that these two structures are separated by 260 kJ mol^{-1}, so we have not considered the triplet structure further. The degenerate stepwise rearrangement of singlet CCCS is shown in Fig. 7, with full details of minima and transition states listed in Table 7. There is no concerted rearrangement of lower energy. The S rearrangement is more favourable than the corresponding O rearrangement of CCCO: CCCS and CCCO require excess energies of ≥ 336 and 479 kJ mol^{-1} respectively to effect rearrangement. Even so, the S rearrangement is highly energetic in accord with the experimental observation that it does not occur under NR conditions. Interestingly, the reaction proceeds through a key rhombic C_3S intermediate (216 kJ mol^{-1} above CCCS), while the corresponding rhombic species in the CCCO rearrangement is a transition state.

The $^-CR^+$ and $^-NR^+$ spectra of $(CC^{13}CS)^{-\bullet}$ show that significant rearrangement occurs within the parent radical cation. The results of molecular modelling the reaction coordinate of the degenerate rearrangement of $(CCCS)^{+\bullet}$ are shown in Fig. 8, with full details of minima and transition states listed in Table 8. The rearrangement is a stepwise process. No lower energy concerted process was found. This stepwise

Table 7 Calculated properties of CCCS neutral species shown in Fig. 7

	C_1–C_2–C_3–S	S, C_1–C_2–C_3	S, C_1–C_2, C_3	C_1, C_2, S, C_3	C_2, C_1, S, C_3
State	$^1\Sigma$	$^1A'$	$^1A'$	$^1A'$	$^1A_1$
Relative energy (kJ mol^{-1})[a]	0.0	336.1	266.2	278.6	216.3
Dipole moment (Debye)[b]	3.04	4.11	2.17	2.52	2.86
C_1C_2 (Å)	1.286	1.281	1.309	1.303	1.420
C_2C_3	1.294	1.420	1.431	1.469	1.473
C_3S	1.551	1.609	1.741	1.788	1.762
C_2S		2.292	1.818	1.740	1.420
$C_1C_2C_3$ (°)	180.0	177.8	159.4	103.9	58.7
C_2C_3S	180.0	98.2	69.1	63.7	65.3
$C_1C_2C_3S$	180.0	0.0	180.0	180.0	180.0

[a] Energies are calculated at the CCSD(T)/aug-cc-pVDZ//B3LYP/6-31G(d) level of theory and are relative to CCCS (−511.5287282 Hartrees). [b] B3LYP/6-31G(d) geometries.

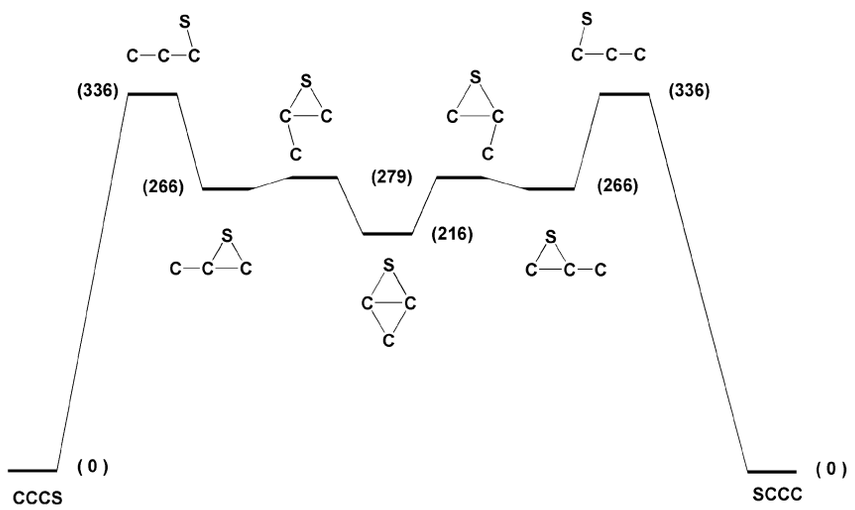

Fig. 7 Degenerate rearrangement of singlet CCCO. Energies [kJ mol^{-1}, relative to CCCS, 0 kJ mol^{-1}] at the CCSD(T)/aug-cc-pVDZ//B3LYP/6-31G(d) level of theory. For details of geometries and energies of minima and transition states see Table 7.

rearrangement is more energetically feasible than any other rearrangements considered in this paper. It is very similar in mechanism to the neutral CCCS rearrangement considered above. The cation requires an excess energy of ≥ 226 kJ mol^{-1} in order to effect the degenerate rearrangement which proceeds through a symmetrical 'rhombic' C_3S cation lying 189 kJ mol^{-1} above CCCS. The neutral and cationic CCCS have very similar geometries (see Tables 6 and 7), thus the excess energy of the cation as a function of the Franck–Condon vertical process will be small. The Franck–Condon excess energy can be calculated since it is the difference in energy between doublet $(CCCS)^{+\bullet}$ and of the cation with neutral geometry on the cationic surface. This energy is only 17 kJ mol^{-1} at the level of theory used in this investigation, hence rearranging $(CCCS)^{+\bullet}$ cations must obtain the additional energy by keV collisions with the collision gas in the collision cell.

The $^-NR^+$ spectrum of $(CC^{13}CS)^{-\bullet}$ is weak in comparison to the $^-CR^+$ spectrum, but it shows an area ratio of close to 3 : 1 for the losses of C and ^{13}C, and 1 : 1 for losses of CC and $C^{13}C$. In the case of $(CC^{13}CS)^{+\bullet}$, the key intermediate is the 'rhombic' structure shown in Scheme 3. This intermediate can ring open to give the two three membered ring systems shown in Scheme 3. Equilibration of this system accompanied by ring opening will give $(CC^{13}CS)^{+\bullet}$, $(C^{13}CCS)^{+\bullet}$ and $(^{13}CCCS)^{+\bullet}$ in the ratio 1 : 1 : 1. This will lead to the decomposition ratios (i) C to ^{13}C loss (2 : 1), and (ii) CC to $C^{13}C$ loss (1 : 2), assuming there is no ^{13}C kinetic isotope effect operating. The experimentally observed ratios indicate that incomplete carbon scrambling accompanies the fragmentations outlined above. The losses of C and CC from $(CCCS)^{+\bullet}$ are both high energy processes [+784 to +581 kJ mol^{-1} respectively (at the CCSD(T)/aug-cc-pVDZ//B3LYP/6-31G(d) level of theory)].

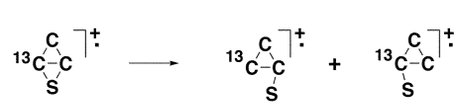

Scheme 3

In conclusion

1 The neutrals CCCO and CCCS can be made by one-electron vertical oxidation of the anion precursors $(CCCO)^{-\bullet}$ and $(CCCS)^{-\bullet}$.

2 The majority of neutrals CCCO and CCCS formed by this Franck–Condon process are stable for at least a microsecond, but a small proportion may decompose to form CC and CO, and S and CCC respectively. Neither oxygen (CCCO to OCCC) nor sulfur rearrangement (CCCS to SCCC) occurs during the NR timeframe.

3 The structures of the neutrals CCCO and CCCS were probed by a consideration of the decompositions of the corresponding cations (produced by ionisation of the neutrals). A minority of the $(CCCO)^{+\bullet}$ cations undergo the degenerate rearrangement to $(OCCC)^{+\bullet}$.

In contrast, the analogous $(CCCS)^{+\bullet}$ to $(SCCC)^{+\bullet}$ rearrangement is significant under NR conditions.

4 The reason why CCCS does not undergo S rearrangement while CCCHS does,[14] is due to the lower energy requirement for rearrangement of CCCHS [CCCHS (+100 kJ mol^{-1});[14] CCCS

Table 8 Calculated properties of $CCCS^{+\bullet}$ species shown in Fig. 8

	C_1–C_2–C_3–S	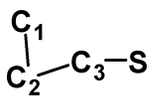	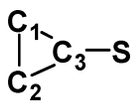	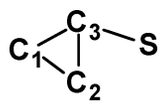	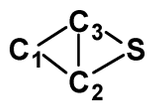
State	$^2\Sigma$	$^2A'$	$^2A_1$	$^2A''$	$^2A_1$
Relative energy (kJ mol^{-1})[a]	0.0	125.8	108.6	225.8	188.5
Dipole moment (Debye)[b]	1.35	1.05	1.08	2.51	0.19
C_1C_2 (Å)	1.227	1.300	1.304	1.521	1.345
C_2C_3	1.336	1.453	1.511	1.554	1.509
C_1C_3		1.632	1.304	1.382	1.345
C_3S	1.510	1.533	1.542	1.646	1.757
C_2S				1.914	1.757
$C_1C_2C_3$ (°)	180.0	72.5	64.5	53.4	55.9
C_2C_3S	180.0	161.2	154.5	73.4	64.6
$C_1C_2C_3S$	180.0	180.0	180.0	180.0	180.0

[a] Energies are calculated at the CCSD(T)/aug-cc-pVDZ//B3LYP/6-31G(d) level of theory and are relative to $CCCS^{+\bullet}$ (−511.1557742 Hartrees). [b] B3LYP/6-31G(d) geometries.

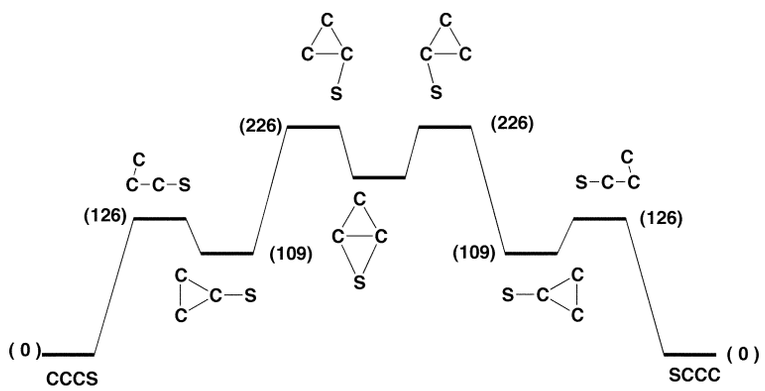

Fig. 8 Degenerate rearrangement of $(CCCS)^{+\bullet}$. Energies [kJ mol^{-1}, relative to $(CCCS)^{+\bullet}$, 0 kJ mol^{-1}] at the CCSD(T)/aug-cc-pVDZ//B3LYP/6-31G(d) level of theory. For details of geometries and energies of minima and transition states see Table 8.

(+ 393 kJ mol^{-1})]. This difference is primarily a consequence of the different geometries of the two systems: for CCCHS and CCCS, the CCS angles are 114.4°[14] and 180° respectively.

Experimental section

A Mass spectrometric methods

For a detailed description of the experiment and the instrument used, see.[13] In brief, the experiments were performed using a two-sector modified VG ZAB 2HF mass spectrometer with BE configuration, where B and E represent magnetic and electric sectors, respectively. The precursor anions to CCCO and CCCS were formed in the chemical ionisation ion source by the SF_6 method[2,35] shown in Scheme 2. Typical source conditions were as follows: source temperature 200 °C, repeller voltage −0.5 V, ion extraction voltage 7 kV, mass resolution m/Δm ≥ 1500. Each neutral precursor was inserted into the ion source through the direct probe which was heated to 60 °C to give a measured pressure of *ca.* 10^{-6} Torr inside the source housing. The reagent gas SF_6 was introduced through a gas inlet into the ion source, to give a measured total pressure of *ca.* 10^{-5} Torr in the source housing. The estimated total pressure in the ion source is 10^{-1} Torr. Collisional induced (CID) spectra of the anions were determined using B to select the parent anion in each case, and utilising argon as the target gas in the first collision cell following B. The pressure of argon in the first cell was maintained such that 80% of the parent ion beam was transmitted through the cell. This corresponds to an average of 1.1–1.2 collisions per ion.[36] Product anion peaks resulting from CID processes were recorded by scanning E.

Neutralisation–reionisation[37–39] ($^-NR^+$) experiments were performed for mass-selected anions utilising the dual collision cells located between the magnetic and electric sectors. Neutralisation of anions was effected by collisional electron detachment using O_2 at 80% transmittance (of the main beam) as the collision gas in the first collision cell, while reionisation to cations was achieved by collision of the neutrals with O_2 (80% transmittance) in the second collision cell. In order to detect a reionisation signal due to the parent neutral, the neutral species must be stable for the one microsecond timeframe of this experiment. Charge reversal ($^-CR^+$) spectra[40,41] were recorded using single collision conditions in collision cell 1 (O_2, 80% transmission of main beam).

B Synthetic procedures

Trimethylsilylpropyn-1-al,[42] and 1,3-bis(trimethylsilyl)-2-propyn-1-one,[42] were made by standard procedures. {3,6-Dihydro-4,5-dimethyl-2-[(trimethylsilyl)ethynyl]-2*H*-thiopyran-2-yl}trimethyl silane (intermediate C, Scheme 1) was also made by a standard procedure,[43] but spectroscopic data was not reported. This compound has the following spectroscopic data:- υ (cm^{-1}), 2155 (C + C); $M^{+\bullet}$, *m*/*z* 296; ^{1}H NMR, δ ($CDCl_3$, 200 mHz): −0.03 (s, 9H, TMS); 0.19 (s, 9H, TMS); 1.12 (m, 2H, CH_2C); 1.51 (s, 3H, CH_3); 1.56 (s, 3H, CH_3); 3.10 (m, 2H, CH_2S).

C Theoretical methods

Geometry optimisations were carried out with the Becke 3LYP method[44,45] using the Dunning aug-cc-pVDZ basis set[46] within the GAUSSIAN 98 suite of programs.[47] Stationary points were characterised as either minima (no imaginary frequencies) or transition structures (one imaginary frequency) by calculation of the frequencies using analytical gradient procedures. The minima connected by a given transition structure were confirmed by intrinsic reaction coordinate (IRC) calculations. The calculated frequencies were also used to determine zero-point vibrational energies which were used as a zero-point correction

for the electronic energies. We have previously reported the success of the B3LYP method in predicting geometries of unsaturated chain structures, and that this method produces optimised structures, at low computational cost, that compare favourably with higher level calculations.[48] The B3LYP method provides good agreement with experimental observations of C_nS (n = 2–9) molecules.[49] More accurate energies for the B3LYP geometries were determined using the CCSD(T) method including zero point energy correction (calculated by vibrational frequencies at the B3LYP/aug-cc-pVDZ level of theory). All calculations were carried out on the Alpha Server at the Australian Partnership for Advanced Computing (APAC) National Facility (Canberra).

Acknowledgements

We thank the Australian Research Council for ongoing funding of our negative ion programme. A.M.McA. thanks the ARC for a research associate stipend. We thank the Australian Partnership for Advanced Computing (APAC) National Facility (Canberra) for a generous allowance of time on their super computing facility.

References

1 S. Dua, S. J. Blanksby, S. Peppe, A. M. McAnoy and J. H. Bowie, *Curr. Org. Chem.*, 2003, **7**, 1545.
2 S. J. Blanksby, D. Schröder, S. Dua, J. H. Bowie and H. Schwarz, *J. Am. Chem. Soc.*, 2000, **122**, 7105.
3 S. Dua and J. H. Bowie, *J. Phys. Chem. A*, 2002, **106**, 1374.
4 S. J. Blanksby, S. Dua, J. H. Bowie, D. Schröder and H. Schwarz, *J. Phys. Chem. A*, 2000, **104**, 11248.
5 H. Olofsson, *Molecules in the Stellar Environment, Lecture Notes in Physics*, ed. O. G. Jorgenson, Springer: Heidelberg, 1994, pp. 114–133 and references cited therein.
6 P. F. Bernath, K. H. Hinkle and J. J. Keady, *Science*, 1989, **244**, 562.
7 K. H. Hinkle, *Molecules in the Stellar Environment, Lecture Notes in Physics*, ed. O. G. Jorgenson, Springer: Heidelberg, 1994, pp. 99–114 and references cited therein.
8 D. Smith and P. Spanel, *Mass Spectrom. Rev.*, 1995, **14**, 255.
9 S. J. Blanksby and J. H. Bowie, *Mass Spectrom. Rev.*, 1999, **18**, 131.
10 Y. Hirahara, Y. Ohshima and Y. Endo, *Astrophys. J.*, 1993, **408**, L113; Y. Kasai, O. Kinichi, Y. Ohshima, Y. Korahara, Y. Endo, K. Kawaguchi and A. Muramaki, *Astrophys. J.*, 1993, **410**, L45.
11 V. Trimble, *Rev. Mod. Phys.*, 1975, **47**, 877.
12 R. D. Brown, *Astrophys. J.*, 1985, **297**, 302; M. Ohishi, H. Suzuki, S. Ishikawa, C. Yamada, H. Kanamori, W. M. Irvine, R. D. Brown, P. D. Godfrey and N. Kaifu, *Astrophys. J.*, 1991, **380**, L39.
13 S. Peppe, S. J. Blanksby, S. Dua and J. H. Bowie, *J. Phys. Chem. A*, 2000, **104**, 5817.
14 S. Peppe, S. Dua, A. M. McAnoy and J. H. Bowie, *J. Phys. Chem. A*, 2003, **107**, 1181.
15 H. E. Matthews, W. M. Irvine, P. Friberg, R. D. Brown and P. D. Godfrey, *Nature*, 1984, **310**, 125.
16 R. D. Brown, F. W. Eastwood, P. S. Elmes and P. D. Godfrey, *J. Am. Chem. Soc.*, 1983, **105**, 6496.
17 R. H. Bateman, J. Brown, M. Lefevre, R. Flammang and Y. N. Haverbeke, *Int. J. Mass Spectrom. Ion Phys.*, 1992, **115**, 205.
18 S. Ekern and M. Vala, *J. Phys. Chem.*, 1997, **101**, 3601.
19 S. J. Blanksby, S. Dua and J. H. Bowie, *Rapid Commun. Mass Spectrom.*, 1999, **13**, 2249.
20 E. Herbst, D. Smith and G. N. Adams, *Astron. Astrophys.*, 1984, **138**, L13.
21 R. D. Brown, P. D. Godfrey, D. M. Cragg, E. H. N. Rice, W. M. Irvine, P. Friberg, H. Suzuki, M. Ohishi, N. Kaifu and M. Morimoto, *J. Astrophys.*, 1985, **297**, 302; R. D. Brown, D. A. McNaughton and K. G. Dyall, *Chem. Phys.*, 1988, **119**, 189; R. G. A. R. Maclagan and P. Sudkeaw, *J. Chem. Soc., Faraday Trans*, 1993, **89**, 3325.
22 M. Moazzen-Ahmalsi and F. Zerbetto, *J. Chem. Phys.*, 1995, **103**, 6343.
23 P. Botschwina, J. Flügge and P. Sebald, *J. Phys. Chem.*, 1995, **99**, 9755.
24 Y. Ohshima, Y. Endo and T. Ogata, *J. Chem. Phys.*, 1995, **102**, 1493; S. J. Blanksby, A. M. McAnoy, S. Dua and J. H. Bowie, *Mon. Not. R. Astron. Soc.*, 2001, **328**, 89.
25 T. Ogata, Y. Ohshima and Y. Endo, *J. Am. Chem. Soc.*, 1995, **102**, 3593.
26 R. D. Brown, P. D. Godfrey, P. S. Elmes, M. Rodler and L. M. Tack, *J. Am. Chem. Soc.*, 1985, **107**, 4112.
27 J. M. Oakes and G. B. Ellison, *Tetrahedron*, 1986, **42**, 6263; J. C. Rienstra-Kiracofe, G. B. Ellison, B. C. Hoffman and H. F. Schaefer, *J. Phys. Chem. A*, 2001, **104**, 2273.
28 R. J. Flores, P. I. Juste, L. Carballeira, C. Estevez and F. Gomez, *Chem. Phys. Lett.*, 2001, **343**, 105.
29 S. Lee, *Chem. Phys. Lett.*, 1997, **268**, 69.
30 J. Szczepanski, R. Hodyss, J. Fuller and M. Vala, *J. Phys. Chem. A*, 1999, **103**, 2975.
31 B. M. Bell, W. L. Avery and A. P. Feldman, *Astrophys. J.*, 1993, **417**, L37.
32 J. D. Peeso, W. D. Ewing and T. T. Curis, *Chem. Phys. Lett.*, 1990, **166**, 307.
33 S. Yamamoto, S. Saito, K. Kavaguch, N. Kaifu, H. Suzuki and M. Ohishi, *J. Astrophys.*, 1987, **317**, L119.
34 R. J. Flores, E. Martinez-Nunez, A. S. Vazquez and F. Gomez, *J. Phys. Chem. A*, 2002, **106**, 8811.
35 P. G. Wenthold, J. Hu and R. R. Squires, *J. Am. Chem. Soc.*, 1994, **116**, 6961.
36 J. L. Holmes, *Org. Mass Spectrom.*, 1985, **20**, 169.
37 C. Wesdemiotis and F. W. McLafferty, *Chem. Rev.*, 1987, **87**, 485.
38 D. V. Zagorevskii and J. L. Holmes, *Mass Spectrom. Rev.*, 1994, **13**, 133; N. Goldberg and H. Schwarz, *Acc. Chem. Res.*, 1994, **27**, 347.
39 For NR nomenclature, see C. A. Schalley, G. Hornung, D. Schröder and H. Schwarz, *Int. J. Mass Spectrom. Ion Processes*, 1998, **172**, 181; D. V. Zagorevskii and J. L. Holmes, *Mass Spectrom. Rev.*, 1999, **18**, 87.
40 J. H. Bowie and T. Blumenthal, *J. Am. Chem. Soc.*, 1975, **97**, 2959; J. E. Szulejko, J. H. Bowie, I. Howe and J. H. Beynon, *Int. J. Mass Spectrom. Ion Phys.*, 1980, **34**, 99.
41 M. M. Bursey, *Mass Spectrom. Rev.*, 1990, **9**, 555.
42 K. J. H. Knuithof, R. F. Schmitz and G. W. Klumpp, *Tetrahedron*, 1983, **39**, 3073; M. Journet, D. Cai, L. M. DiMichele and R. D. Larsen, *Tetrahedron Lett.*, 1998, **39**, 6429.
43 A. Degl'Innocenti, A. Capperucci, P. Scafato, T. Mecca, A. Mordini and G. Reginato, *Phosphorus, Sulfur Silicon*, 1999, **153/154**, 321.
44 A. D. Becke, *J. Chem. Phys.*, 1993, **98**, 5648.
45 P. J. Stevens, F. J. Devlin, C. F. Chablowski and M. J. Frische, *J. Phys. Chem.*, 1994, **98**, 11623.
46 T. H. Dunning, *J. Chem. Phys.*, 1989, **90**, 1007; D. E. Woon and T. H. Dunning, *J. Chem. Phys.*, 1993, **98**, 1358; T. H. Dunning, K. A. Peterson and D. E. Woon, Basis Sets: Correlation Consistent, in *Encyclopedia of Computational Chemistry* : P. v R. Schleyer, Ed; Wiley: Chichester, 1998.
47 M. J. Frisch, G. W. Trucks, H. B. Schlegel, G. E. Scuseria, M. A. Robb, J. R. Cheeseman, V. G. Zakrzewski, J. A. Montgomery, R. E. Stratmann, J. C. Burant, S. Dapprich, J. M. Millam, A. D. Daniels, K. N. Kudin, M. C. Strain, O. Farkas, J. Tomasi, V. Barone, M. Cossi, R. Cammi, B. Mennuchi, C. Pomelli, C. Adamo, S. Clifford, J. Ochterski, G. A. Pedersson, P. Y. Ayala, Q. Cui, K. Morokuma, D. K. Malick, A. D. Rabuck, K. Raghavachari, J. B. Foresman, J. Cioslowski, J. V. Ortiz, A. G. Baboul, B. Stefanov, G. Liu, M. A. Al-Latam, C. Y. Peng, A. Nanayakkara, M. Chalacombe, P. M. W. Gill, B. Johnson, W. Chem, M. W. Wong, J. L. Andres, C. Gonzales, M. Head-Gordon, E. S. Replogle, J. A. Pople, *Gaussian 98*; Revision A.9 ed.; Gaussian Inc., Pittsburgh, PA, 1998.
48 S. J. Blanksby, S. Dua and J. H. Bowie, *J. Phys. Chem.*, 1999, **103**, 5161. To cite a particular example, the value of adiabatic electron affinity of CCCC was calculated to be 3.65 eV at the same level of theory used in this study, while the experimental value is 3.88 eV^2.
49 S. Lee, *Chem. Phys. Lett.*, 1997, **268**, 69.